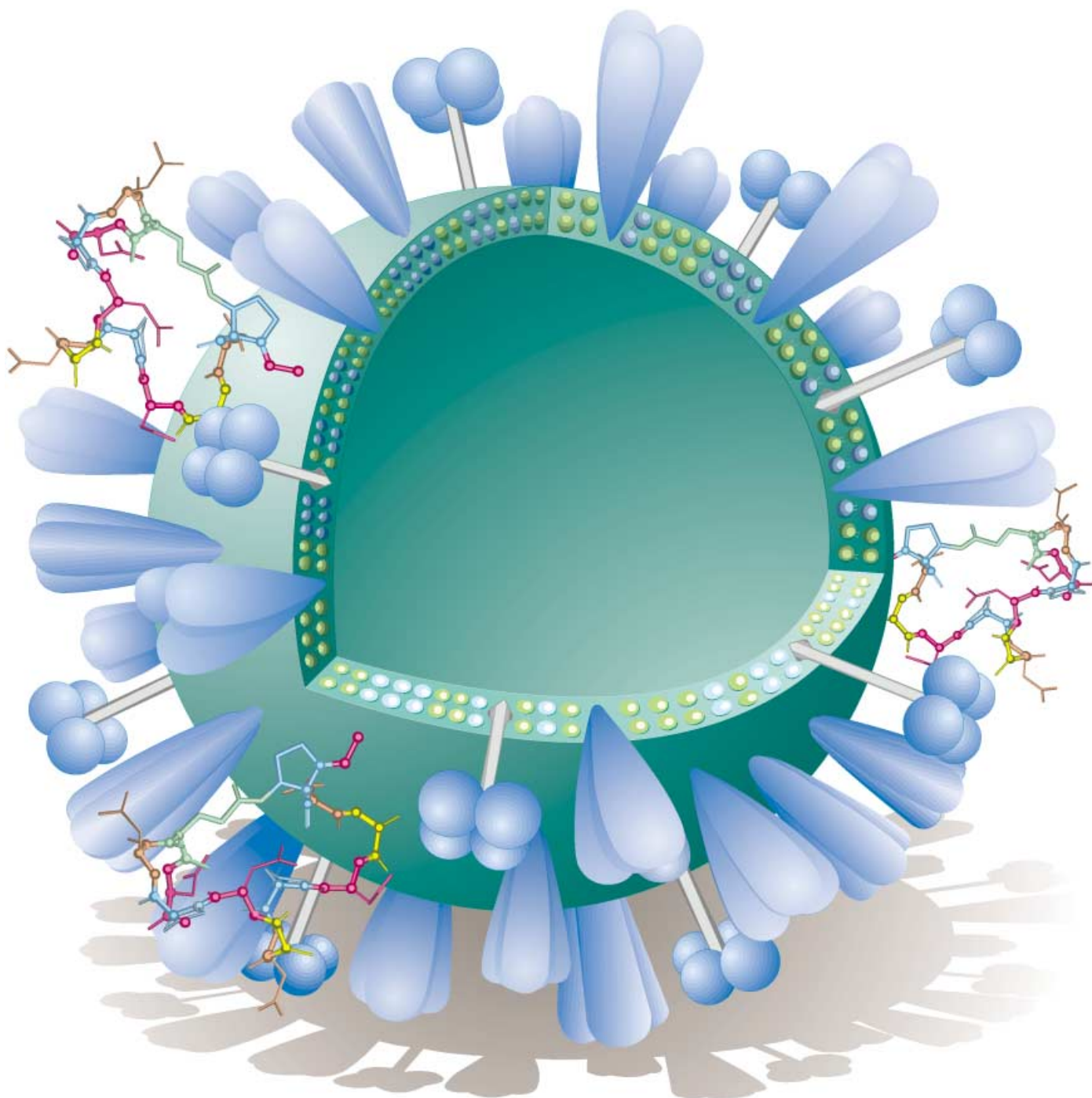


Communications



Making the influenza virus look more like the malaria parasite could have important implications for synthetic-vaccine design. New synthetic mimotopes displayed on virosomes elicit a strong antibody response against the malaria parasite *P. falciparum*. For more information see the following Communication by Pluscke, Robinson, and co-workers.

Peptidomimetic Vaccine Design

A Virosome-Mimotope Approach to Synthetic Vaccine Design and Optimization: Synthesis, Conformation, and Immune Recognition of a Potential Malaria-Vaccine Candidate

Bernhard Pfeiffer, Elisabetta Peduzzi, Kerstin Moehle, Rinaldo Zurbriggen, Reinhard Glück, Gerd Pluschke,* and John A. Robinson*

Attempts to produce a vaccine against the malaria parasite *Plasmodium falciparum* have so far met with limited success. The molecules used to stimulate a protective antibody response have in general shown only poor efficacy in humans.^[1] Synthetic peptides are attractive targets for vaccine design, as they are readily synthesized and are able to target specific antigens, but their use has suffered a number of drawbacks.^[2] These include poor immunogenicity and poor mimicry of conformational epitopes, poor proteolytic stability, and the lack of a suitable delivery system in humans. To enhance immunogenicity, short peptides are usually coupled to a carrier protein and then injected together with an immunostimulatory adjuvant, which for humans is typically an alum-absorbed antigen.

We introduce herein an alternative approach to synthetic-vaccine design and optimization (see Figure 1), which involves the use of peptidomimetics delivered to the immune system on the surface of immunopotentiating reconstituted influenza virosomes (IRIVs).^[3] The IRIVs are similar to liposomes, but contain influenza-derived, membrane-bound hemagglutinin and neuraminidase, which impart fusogenic activity and facilitate antigen delivery to immunocompetent cells. The potential advantages of IRIVs for vaccine delivery include their fusogenic activity, the surface display of molecularly defined antigens, and compatibility with both animals (e.g. mice) and humans.^[4] Sequential rounds of mimetic optimization based on structure–activity relationships may ideally lead to vaccine candidates, which after appropriate preclinical profiling, can be tested in human

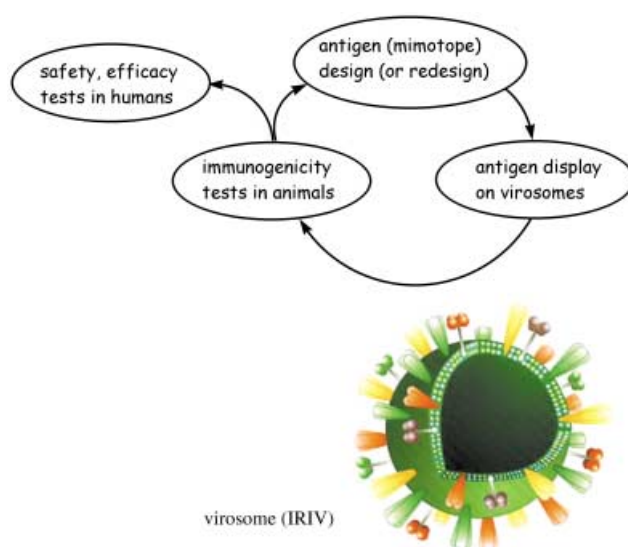


Figure 1. Using virosome technology, sequential cycles of design, testing and optimization of peptidomimetics in animal models can be followed by human clinical trials with the same molecularly defined adjuvant/delivery system.

clinical trials.^[5] It is expected that the extensive clinical experience obtained with two IRIV-based vaccines already licensed^[5] will facilitate the development of new IRIV-mimotope vaccine candidates. We illustrate this approach herein with a model system comprising the NPNA-repeat epitope from *Plasmodium falciparum*.

One of the early synthetic malaria-vaccine candidates to be tested in humans was a linear (NANP)₃ peptide conjugated to tetanus toxin in alum.^[6] This peptide mimics epitopes in the central repeat region (NPNA)_{≈37} of the major surface protein on sporozoites, the circumsporozoite (CS) protein.^[7,8] However, the efficacy of this construct in humans was poor. Building on these earlier studies, we describe below an improved NPNA mimetic incorporated into IRIVs and its potential as a new malaria-vaccine candidate.

A key step in the design of the new mimetic evolved from earlier studies^[9] of **1** (Figure 2) as well as of linear (NPNA)_n

[*] Prof. J. A. Robinson, Dr. B. Pfeiffer, Dr. K. Moehle
Institute of Organic Chemistry, University of Zurich
8057 Zurich, Winterthurerstrasse 190, 8057 Zürich (Switzerland)
Fax: (+41) 1-635-6833
E-mail: robinson@oci.unizh.ch

Prof. G. Pluschke, E. Peduzzi
Swiss Tropical Institute
Socinstrasse 57, 4002 Basel (Switzerland)
Fax: (41) 1-61-271-8654
E-mail: Gerd.Pluschke@unibas.ch

Dr. R. Zurbriggen
Pevion-Biotech
Rehhagstrasse 79, 3018 Bern (Switzerland)

Dr. R. Glück
Berna-Biotech
Rehhagstrasse 79, 3018 Bern (Switzerland)

Supporting information for this article is available on the WWW under <http://www.angewandte.org> or from the author.

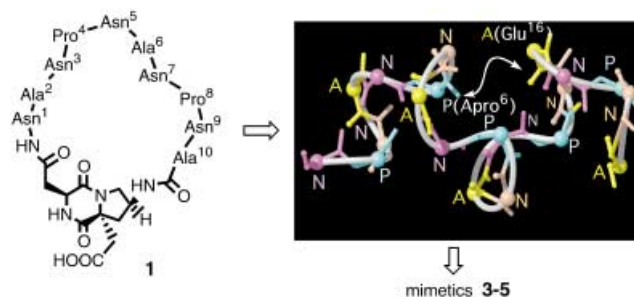
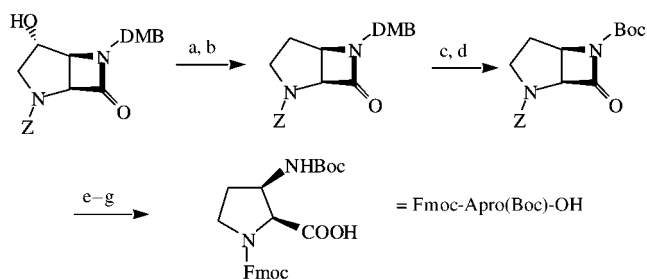


Figure 2. Mimetic **1** and a computer model of Ac-(NPNA)₅-NH₂ with a backbone conformation in which each NPNA motif adopts a helical β turn (see text). The arrows indicate the position of the proposed amide cross-link between (2S,3R)-3-aminoproline (Apro, residue 6) and glutamic acid (Glu, residue 16). Color coding: Asn = pink, Pro = cyan, Ala = yellow. The C α atoms are each marked along the ribbon with a ball.

peptides.^[10] Modeling and NMR spectroscopic studies suggested^[9] that the central NPNA motif in **1** may adopt conformations in which the first Asn residue is in the β region of ϕ/ψ space (e.g. $-120/+120^\circ$) and the next three residues Pro–Asn–Ala are each in the helical region (e.g. $-60/-40^\circ$). Based on these ϕ/ψ angles, a computer model was built for the linear sequence Ac-(NPNA)₅-NH₂, such that this helical turn is tandemly repeated. The resulting model (which differs from previously reported theoretical models^[11–13]) was stable in molecular-dynamics simulations (data not given), and displays a novel repetitive secondary structure (see Figure 2). Examination of the model suggested that this folded conformation could be stabilized by cross-linking an amino group at the β position of Pro6 to a spatially adjacent side-chain carboxy group of Glu, to be used in turn as a replacement for Ala16. This would require cyclic peptidomimetics **3–5** (Scheme 2), containing (2*S*,3*R*)-3-aminoproline (Apro)^[16] at position 6 and glutamate at position 16 (Figure 2), linked by an amide bond. The required orthogonally protected (2*S*,3*R*)-3-aminoproline was prepared as shown in Scheme 1

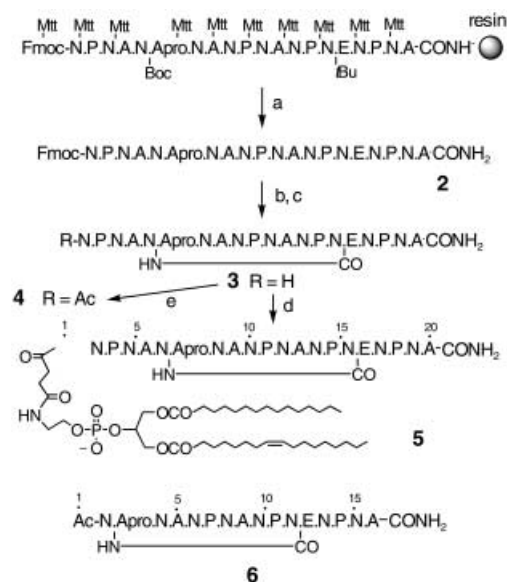


Scheme 1. Reagents and conditions: a) (CF₃SO₂)₂O, CH₂Cl₂, pyridine, 98%; b) NaBH₄, THF/DMF, 58%; c) K₂S₂O₈, Na₂HPO₄, MeCN/H₂O, 80%; d) (Boc)₂O, CH₂Cl₂, DMF, Et₃N, 76%; e) LiOH, THF, H₂O, 99%; f) Pd/C, MeOH, H₂, 93%; g) Fmoc-OSucc, *i*Pr₂NEt, CH₂Cl₂, 68%. Apro = (2*S*,3*R*)-3-aminoproline; Boc = *tert*-butyloxycarbonyl; DMB = 3,4-dimethoxybenzyl; DMF = *N,N*-dimethylformamide; Fmoc = 9-fluorenylmethoxycarbonyl; Succ = succinimide.

The mimetic **4** and an analogue **5**, which was linked to a phospholipid for incorporation into IRIVs, were synthesized as shown in Scheme 2. The linear sequence was built through solid-phase Fmoc chemistry on Rink-amide MBHA resin (*Novabiochem*). After cleavage from the resin, the 3-amino group of Apro6 and the carboxy group of Glu16 could be coupled in high yield (> 90%) in DMF in the presence of HATU.

The conformation of **4** was studied by NMR spectroscopy in H₂O/D₂O (9:1) at pH 5. ¹H NMR spectra indicated the existence of a major conformer and two minor conformers (ratio 80:14:6), of which the latter two most likely arise from *cis*–*trans* isomerism at Asn–Pro peptide bonds, in analogy to earlier studies.^[10,14,15]

Only the major form of **4** was considered further. 2D NOESY plots showed strong $d_{\text{NN}}(i, i+1)$ connectivities between the peptide NH groups of Asn 7 and Ala 8, and Ala 8 and Asn 9 in one NPNA motif, Asn 11 and Ala 12, and Ala 12 and Asn 13 in the next, and between Asn 15 and Glu 16, and Glu 16 and Asn 17 in the last motif. These, together with



Scheme 2. Synthesis of mimetics. a) TFA, *i*Pr₃SiH, H₂O (95:2.5:2.5); b) HATU, HOAt, DMF, *i*Pr₂EtN; c) piperidine, DMF (20% v/v); d) succinyl-*rac*-1-palmitoyl-3-oleoyl-glycero-2-phosphoethanolamine, HATU, HOAt, *i*Pr₂EtN; e) Ac₂O, pyridine/CH₂Cl₂. HATU = 2-(1*H*-7-azabenzotriazol-1-yl)-1,1,3,3-tetramethyluronium hexafluorophosphate; HOAt = 1-hydroxy-7-azabenzotriazole; Mtt = 4-methyltrityl; TFA = trifluoroacetic acid.

NOE interactions between Pro C α -H and Ala N-H (*i*+2) in each motif, provide evidence for helical turns formed by the residues Asn5–Asn9, Asn9–Asn13, and Asn13–Asn17. The same pattern of NOE interactions was also found for **6** (Scheme 2). Signal overlap of side-chain resonances seen in the NMR spectrum of **4** was less severe for **6**. Mimetics **4** and **6** showed similar coupling patterns of ³*J*(C α -H, N-H) and amide-proton temperature coefficients (see Supporting Information) in their common substructures. However, the amide temperature coefficients were mostly more negative than -4 ppb/K and all the amide protons in **4** and **6** exchanged within a few minutes at pH 4 in D₂O, which suggests the absence of stable intramolecular hydrogen bonds involving the amide NHs.

Average solution structures were calculated for **4** and **6** by simulated annealing based on NOE-derived distance restraints, and gave similar results, except for the very flexible N- and C-termini in **4**. For example, the average structures for **6** could be clustered into four main families, as depicted in Figure 3 (see Supporting Information). The lack of convergence to a single structure reflects a low number of long range NOE restraints, which we presume is a result of significant backbone flexibility, compounded by problems of signal overlap. However, in some of the calculated structures the anticipated helical turns are populated (see Figure 4).

For immunological studies, the mimetic **5** was incorporated into IRIVs and then used to immunize BALB/c mice. After preimmunization with the IRIV-based influenza vaccine Inflexal Berna^[17] (Berna Products), and three doses of **5**-IRIV, the sera of all immunized mice contained mimetic-specific antibodies, as demonstrated by ELISA (enzyme-

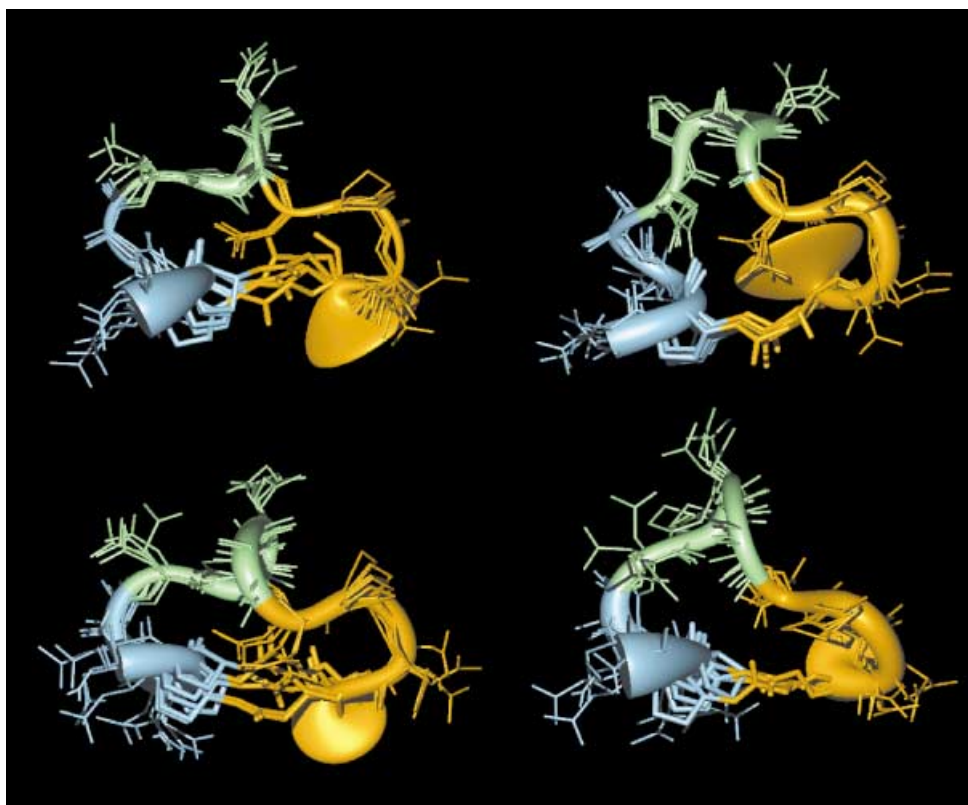


Figure 3. Average solution structures for **6** (Scheme 2). The calculated structures cluster into four main groups as shown. The sausage-shaped average backbone was calculated from the average displacement of the C_{α} atoms, which is represented by the spline radius. The first helical NPNA turn is in blue, the second in green, and the third in orange. The Apro6–Glu16 cross-link is at the bottom of the structure. The figure was prepared with MOLMOL.^[20]

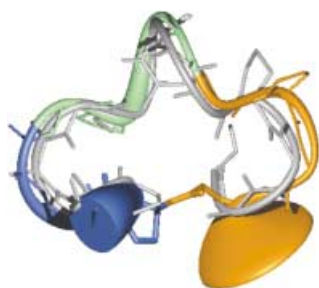


Figure 4. Superimposition of the computer model of $Ac-(NPNA)_5-NH_2$ shown in Figure 2 and average solution structures for **6** shown in Figure 3.

linked immunosorbent assay) (Figure 5a). The binding of anti-**5**-IRIV antisera to native circumsporozoite (CS) protein was analyzed by an indirect immunofluorescence assay using *P. falciparum* sporozoites. In all immunized animals a significant antisporozoite antibody response was detected. The specificity of the cross-reaction was demonstrated by a competition experiment (Figure 5b). Incubation of the antiserum with the sporozoites in the presence of **4** completely suppressed immunostaining. The IRIV formulations thus elicited a significant proportion of parasite-binding antibodies among the total antimimetic immune response. Priming of mice with influenza antigens has been found to enhance the

humoral immune response against antigens delivered by virosomes.^[5,18] Primed mice presumably reflect the situation in humans better than nonprimed mice, as most humans are already exposed to the influenza virus early in life. Currently it is not clear whether influenza antigen-specific helper T cells or antibodies are primarily responsible for the effects of influenza preimmunity.

The cross-reactivity of the antisera with peptidomimetic **1** was also analyzed by ELISA (data not shown). The sera from three of four mice immunized with **5**-IRIV cross-reacted with mimetic **1**. Interestingly, a helical NPNA turn (see above) is also possible in **1**.^[9] That a significant part of the antibody response to **5**-IRIV cross-reacts with **1** also shows that these cross-reacting antibodies must not simply recognize the ends of the peptide backbone in **5**.

Monoclonal antibodies (mAbs) were prepared from spleen cells of mice immunized with **5**-IRIV, and two mAbs (EP3 and EP9) that bound both the mimetic **5**-IRIV and *P. falciparum* sporozoites were isolated. Both EP3 and EP9 have recently also been shown to inhibit the invasion of human-liver hepatocytes by live sporozoites in the midnanomolar range.^[19] This inhibitory activity most likely arises as a result of binding by the mAbs of neutralizing epitopes on the parasite surface.

The cross-reactivity of EP3 and EP9 with peptidomimetic **1** and the linear peptide $(NANP)_{\approx 50}$ were also tested by ELISA. The results show that both EP3 and EP9 bind to **1**,

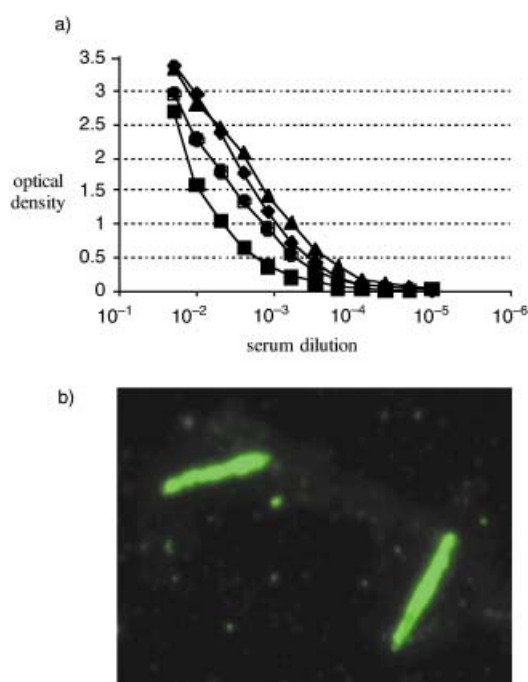


Figure 5. a) Serum IgG titers in BALB/c mice immunized three times with 5-IRIV. ELISA was performed in microtiter plates coated with 5 and incubated with serial dilutions of the sera of individual mice. Bound IgG was detected using alkaline phosphatase-conjugated antibodies specific for mouse gamma heavy chains. No antibody binding was observed with uncoated plates and preimmune sera exhibited no significant antimimotope antibody titer in ELISA (data not shown). b) Immunofluorescence staining of *P. falciparum* sporozoites by mouse anti-5-IRIV antiserum, using a FITC-labeled secondary anti-mouse IgG antibody. No significant staining was observed with preimmune sera and incubation of the sporozoites in the presence of 4 suppressed immunostaining (data not shown). FITC = (fluorescein isothiocyanate).

whereas (NANP)_{~50} is only bound by EP9 and not by EP3 in ELISA. These data suggest that EP3 recognizes epitopes in both 5-IRIV and on the parasite surface that are more poorly represented, if at all, in the linear peptide (NANP)_{~50}.

The results show that the IRIV-bound peptidomimetic 5 effectively elicits sporozoite-binding antibodies, and also lead to a new proposal for the folded conformation of the NPNA-repeat region in the CS protein (Figure 2). A key issue now is whether the use of this peptidomimetic with the IRIV delivery system leads to a stronger antiparasite immune response in humans than in mice, as has been observed with other virosome-based vaccine candidates. In this case, influenza preimmunity may play a role, as suggested by the enhancing effects of influenza priming in mice. The suitability of virosomal mimetic formulations for use in humans will have to be evaluated in a phase I clinical safety and immunogenicity trial. At a later stage, efficacy trials will reveal whether the IRIV-based vaccine candidate offers improvements in protective efficacy over linear (NANP)₃ peptides delivered by the classical route.^[6] The virotope approach, however, could also be applied to the design and testing of new combination vaccines targeted against multiple

antigens and developmental stages of *P. falciparum*, or indeed against other infectious agents.

Received: October 11, 2002

Revised: January 31, 2003 [Z50348]

Keywords: antibodies · conformation analysis · immunochemistry · peptides · peptidomimetics

- [1] M. Tsuji, E. G. Rodrigues, R. S. Nussenzweig, *Biol. Chem.* **2001**, 382, 553.
- [2] *Ciba Foundation Symposium 119: Synthetic Peptides as Antigens* (Eds.: R. Porter, J. Whelan), Wiley, Chichester, UK, **1986**.
- [3] R. Glück, *Vaccine* **1999**, 17, 1782.
- [4] I. P. Hunziker, R. Zurbriggen, R. Glueck, O. B. Engler, J. Reichen, W. J. Dai, W. J. Pichler, A. Cerny, *Mol. Immunol.* **2001**, 38, 475.
- [5] R. Zurbriggen, R. Glück, *Vaccine* **1999**, 17, 1301.
- [6] D. A. Herrington, D. F. Clyde, G. Losonsky, M. Cortesia, J. R. Murphy, J. Davis, S. Baqar, A. M. Felix, E. P. Heimer, D. Gillissen, E. Nardin, R. S. Nussenzweig, V. Nussenzweig, M. R. Hollingdale, M. M. Levine, *Nature* **1987**, 328, 257; for other examples, see reference [1].
- [7] F. Zavala, J. P. Tam, M. R. Hollingdale, A. H. Cochrane, I. Quakyi, R. S. Nussenzweig, V. Nussenzweig, *Science* **1985**, 228, 1436.
- [8] J. B. Dame, J. L. Williams, T. F. McCutchan, J. L. Weber, R. A. Wirtz, W. T. Hockmeyer, W. L. Maloy, J. D. Haynes, I. Schneider, D. Roberts, G. S. Sanders, E. P. Reddy, C. L. Diggs, L. H. Miller, *Science* **1984**, 225, 593.
- [9] R. Moreno, L. Jiang, K. Moehle, R. Zurbriggen, R. Glück, J. A. Robinson, G. Pluschke, *ChemBioChem* **2001**, 2, 838.
- [10] H. J. Dyson, A. C. Satterthwait, R. A. Lerner, P. E. Wright, *Biochemistry* **1990**, 29, 7828.
- [11] K. D. Gibson, H. A. Scheraga, *Proc. Natl. Acad. Sci. USA* **1986**, 83, 5649.
- [12] I. K. Roterman, K. D. Gibson, H. A. Scheraga, *J. Biomol. Struct. Dyn.* **1989**, 7, 391.
- [13] B. R. Brooks, R. W. Pastor, F. W. Carson, *Proc. Natl. Acad. Sci. USA* **1987**, 84, 4470.
- [14] C. Bisang, C. Weber, J. Inglis, C. A. Schiffer, W. F. van Gunsteren, I. Jelesarov, H. R. Bosshard, J. A. Robinson, *J. Am. Chem. Soc.* **1995**, 117, 7904.
- [15] C. Bisang, L. Jiang, E. Freund, F. Emery, C. Bauch, H. Matile, G. Pluschke, J. A. Robinson, *J. Am. Chem. Soc.* **1998**, 120, 7439.
- [16] For the starting bicyclic lactam, see: P. Angehrn, R. L. Charnas, K. Gubernator, E.-M. Gutknecht, C. Hubschwerlen, M. Kania, C. Oefner, M. G. P. Page, S. Sogabe, J.-L. Specklin, F. Winkler, *J. Med. Chem.* **1998**, 41, 3961–3971.
- [17] R. Glück, R. Mischler, B. Finkel, J. U. Que, B. Scarpa, S. J. Cryz, *Lancet* **1994**, 344, 160.
- [18] F. Poltl-Frank, R. Zurbriggen, A. Helg, F. Stuart, J. A. Robinson, R. Glück, G. Pluschke, *Clin. Exp. Immunol.* **1999**, 117, 496–503.
- [19] Full details of the immunological data will be published elsewhere.
- [20] R. Koradi, M. Billeter, K. Wüthrich, *J. Mol. Graphics* **1996**, 14, 51–55.